Structural Eng./Earthquake Eng., JSCE, Vol. 20, No. 1, 43s—54s, 2003 April
(J. Struct. Mech. Earthquake Eng., JSCE, No. 731/ I —63)

MESO-SCOPIC NUMERICAL ANALYSIS OF CONCRETE STRUCTURES BY A MODIFIED LATTICE MODEL

Mitsuteru ASAI[1], Kenjiro TERADA[2], Kiyohiro IKEDA[3], Hiroyuki SUYAMA[4] and Katashi FUJII[5]

[1]Member of JSCE, M.Eng., Grad. Student, Dept. of Civ. Engrg., Tohoku Univ.
(Aza-Aoba 06 Aramaki, Aoba-ku, Sendai 980-8579, Japan)
[2]Member of JSCE, Ph.D., Associate Professor, Dept. of Civ. Engrg., Tohoku Univ.
[3]Member of JSCE, Ph.D., Professor, Dept. of Civ. Engrg., Tohoku Univ.
[4]M.Eng., Mitsui-kyodo Structural Consultant
(Takada-Baba 1-4-15, Sinjyuku-ku, Tokyo 169-0075, Japan)
[5]Member of JSCE, Dr. Eng., Associate Professor, Dept. of Civ. Engrg., Hirohima Univ.
(Kagamiyama 1-4-1, Higashi-hiroshima 739-8527, Japan)

Realistic simulation of the mechanical behavior of concrete and reinforced concrete structures is performed by using a lattice type numerical model. Five different types of lattice members with simple constitutive models are introduced for mortar, coarse aggregate, steel, aggregate-mortar interface and steel-concrete interface. The meso-scopic morphology of concrete, which can be realized by the image-based geometry modeling technique, is taken into account. By the incorporation of the accurate meso-scopic morphology into the lattice type numerical modeling, the cracking behavior induced by the meso-scopic heterogeneities has been successfully captured.

Key Words : *lattice model, RC-structures, heterogeneous material, strong discontinuity*

1. INTRODUCTION

Concrete, which consists of various materials, displays complex quasi-brittle failure characteristics associated with the local (or meso-scale) *heterogeneities* and the *localization* behavior with micro-scale cracking. In particular, the mechanism of its compressive and shear fracture observed prior to failure is still far from being fully understood. Inevitably, it is quite difficult to analyze the overall behavior of concrete structures in consideration of the meso-scopic heterogeneities, which are often represented by mortar and aggregates.

In this context, it is widely recognized, especially in computational studies, that the hierarchy of material characterization for concrete structures plays a vital role in the successful modeling and analysis of their overall behavior. For example, Zaitsev and Wittmann[1] posed four hierarchical levels of numerical concrete models: including, macro-, meso-, micro- and nano-levels, as shown in **Fig. 1**. While the micro- and nano-scopic levels are related to the physical properties of mortar and coarse aggregates as well as their interface, it is usually understood that the mechanical behavior of overall concrete structures can be characterized on the macro- and meso-scopic levels. In general, the macro-scopic modeling is employed for the structural analysis of an overall concrete structure, whereas the meso-scopic modeling is used to obtain a constitutive relation for the macro-scale analysis.

In macro-scopic models, it is conventional to regard concrete as a homogeneous material and to formulate the governing equations within the framework of continuum mechanics. The so-called smeared crack model serves as a typical example of such models; see, e.g., Bhatt and Abdel-Kader[2] and An and Maekawa[3]. The aim of macro-level analysis is mainly to predict the overall failure condition, such as ultimate loads and load–displacement curves, at low computational cost. It is, however, pointed out that the modeling of discontinuity in displacement, as well as in stress and strain, is not straightforward; see the crack band model by Bažant and Oh[4] and many others.

On the other hand, meso-scopic models deal mainly with local structures composed of coarse aggregates and mortar matrix. In these models, the meso-scopic heterogeneities can be easily incorporated into the complex macro-scopic mechanical responses, such as the size effect of

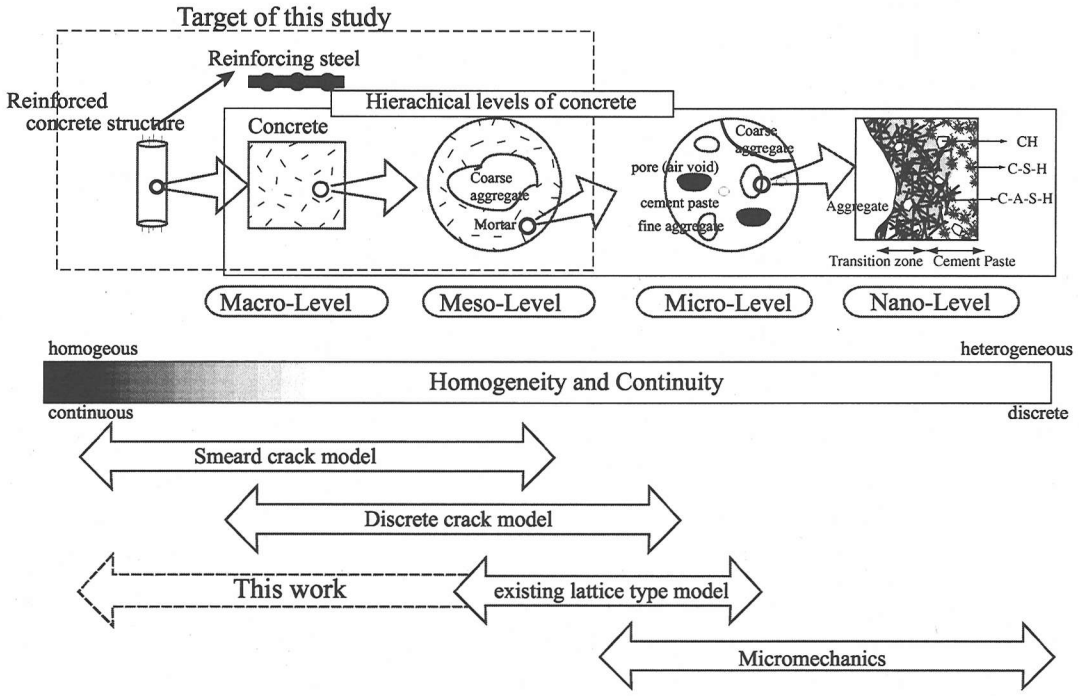

Fig. 1 Structural scales and simulation models for concretes and reinforced concrete structures

un-notched specimens under tension. A representative example of those models is a class of lattice type numerical models, in which the fracture mechanism associated with the meso-scopic heterogeneities is directly implemented by means of simple structural members, such as trusses or beams; see Bažant et al.[5] and Schlangen and van Mier[6]. Several continuum-based and discrete models have been also introduced to characterize the meso-scopic mechanical behavior; see, for example, Nagai et al.[7] for the former and Kwan et al.[8] for the latter.

Although the macro- and meso-scopic models are capable of simulating separate aspects of the mechanical behavior of concrete structures to some extent, each model stays within its own usage, and there have been few attempts to combine these models. In particular, the material characterization in a meso-scale has not been reflected on the simulation of the overall macro-scopic mechanical behavior of concrete structures.

The goal of this study is to simulate the macro-scopic mechanical behavior of concrete- and reinforced concrete structures, which reflects the meso-scopic heterogeneities; see **Fig. 1**. We employ the lattice type model to realize the discrete deformation in meso-scale and, in turn, to capture the cracking behavior and the bond-slip phenomenon between concrete and steel. For this purpose, we annex the following two features to the conventional lattice type modeling:

1. The actual meso-scopic heterogeneities are reflected with the use of the image data of the local morphology of concrete.
2. Five different types of lattice members with simple constitutive models are employed for mortar, aggregate, steel, aggregate-mortar interface and steel-concrete interface.

The proposed numerical concrete model enables us to simulate crack propagation and debonding of aggregate-mortar or concrete-steel interface without introducing any macro-scopic phenomenological constitutive model determined by experiments. To illustrate the performance of the model, we employ two representative numerical examples including (1) the simulation of biaxial test of concrete specimens and (2) the demonstration of the effect of shear reinforcements on the crack formation in reinforced concrete beams.

2. LATTICE TYPE NUMERICAL MODELING

In order to simulate the mechanical behavior of concrete and reinforced concrete structures, the existing lattice type models are modified in this section. After summarizing the features of the existing lattice type models, we explain in

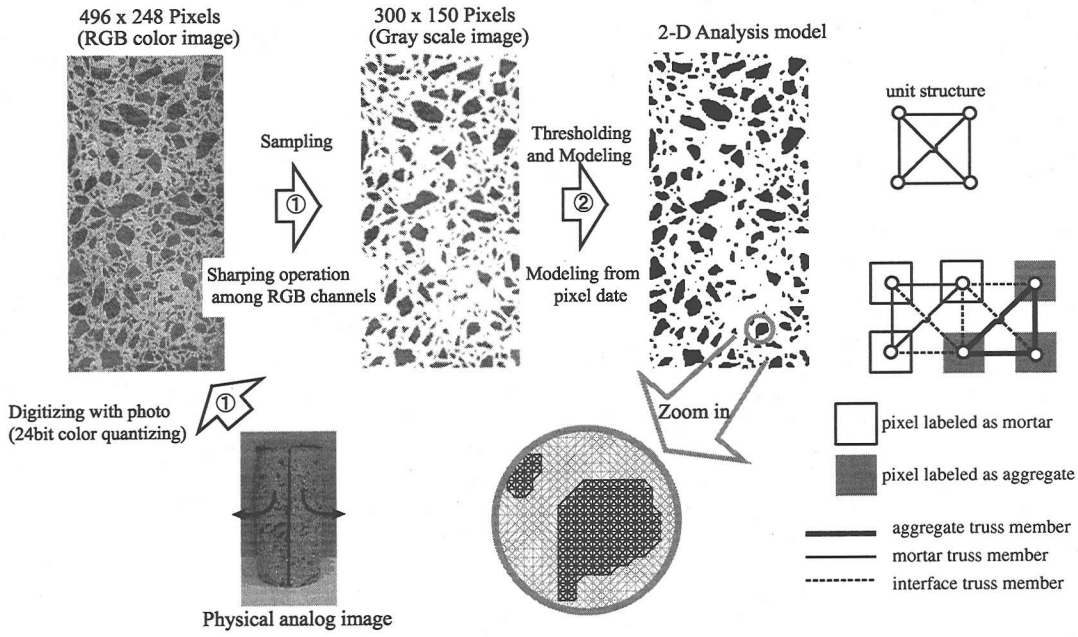

Fig. 2 Procedure of DIB (Digital Image-Based) modeling for lattice type models

detail two major modifications introduced in our modeling.

(1) Existing lattice type models

The lattice type model is first developed from the distinct element method (DEM), which was proposed by Cundall and Strack[9], to simulate the meso-scopic behavior of granular solids. A macro-scopic continuum is discretized as a network of structural members, such as truss or beam elements. This modeling strategy has been extended to simulate the crack growth of concrete with quasi-brittle material properties; see, e.g., Zubelewicz[10] and Zubelewicz and Mróz[11]. These lattice type models fail to incorporate the meso-scale heterogeneities of concrete, and did not employ a series of constitutive models for lattice members.

In meso-scopic numerical analysis, overall structural responses depend heavily on the geometry model that defines the shapes of aggregates and their spatial distributions. In the lattice type modeling, the meso-scopic heterogeneities of concrete are taken into account by randomly scattering circular aggregates. Then, each of the circular aggregate is mapped on a triangular regular lattice network in one case [Schlangen and van Mier[6]]. In another case, which is called the particle model, these aggregates are connected to adjacent ones by pin-jointed trusses at the centers [Bažant et al.[5]]. It may be, however, open to criticism that the use of circular aggregates is too artificial and ideal, while the actual irregular shape could possibly be a source of size effects and complex overall behavior. Therefore, more realistic representation for the meso-scopic morphology is indispensable in the numerical simulations of concrete structures by lattice type models.

In addition, especially in the particle model, the one-dimensional constitutive relationship of lattice members is usually accompanied with the reduction of stiffness based on softening plasticity, in view of the macro-scopic response of concrete material. However, as will be made clear in the numerical simulation, it is sufficient to consider the failure due to tensile loading in meso-scale modeling with lattice network.

(2) Digital image-based modeling

In this study, concrete is assumed to consist of coarse aggregates, mortar matrix and interface regions. That is, concrete is modelled as a two-phase material with the meso-level heterogeneities, whereas we neglect the effects of other constituents in the micro-level, such as fine aggregates, cement paste and air space. By virtue of this assumption, at least the geometrical characteristics of aggregates as well as their spatial distributions are reflected on our modeling.

In order to generate the realistic geometry model for the two-phase material, we employ the digital image-based (DIB) modeling, which was

developed in the studies of computational homogenization; see Hollister and Kikuchi[12] and Terada et al.[13]. The geometry model is constructed in such a way that one pixel in the 2-D case (or one voxel in the 3-D case) is regarded as a single finite element (FE). The same modeling scheme can be directly applied to the modeling of the meso-scopic morphology of concrete, although the lattice approximation for continuous phases necessitates slight modification. In this particular situation for lattice modeling, a pixel is regarded as a hinge labeled by mortar or aggregate and each truss member is characterized as shown in **Fig. 2**. As a result, the modeling is similar to the aforementioned modeling with triangular regular lattice network [Schlangen and Garboczi[14]]. The whole procedure of this modeling can be divided into two major stages: (1) *sampling* and (2) *thresholding* and *modeling*, as schematically shown in **Fig. 2**; see Terada et al.[13] for details.

(3) Meso-scopic constitutive model for each material

An overall analysis model consists of five types of materials: mortar, coarse aggregate, steel, aggregate-mortar interface and steel-concrete interface. Each material is represented by a truss finite element with a simple constitutive model. In the following subsections, our modeling strategy for the meso-scopic material characteristics for each material is presented in order. Note, however, that the mechanical behavior characterized by this modeling depends on the orientation of the unit structure defined in **Fig. 2**. Therefore, the resulting averaged material properties are regarded as apparent ones; e.g., averaged Poisson's ratio of this unit structure is evaluated as 0.22 in this particular setting.

a) Mortar, aggregate and aggregate-mortar interface

In the meso-scopic level, concrete will exhibit elastic-brittle behavior and re-distribute internal force at the onset of brittle failure. Such brittle behavior is caused by the propagation of microcracks and, in turn, new mocrocracks are generated by re-distributed internal forces. Such behavior represents nothing but a geometrical change of structure, but can be viewed as strain softening behavior from the macro-scopic viewpoint. In other words, the macroscopic strain softening behavior is a consequence of local instability, triggered by the progress of the microcrack. This type of macroscopic material response is sometimes called geometrical softening; see Drescher and Vardoulakis[15]. Special attention is paid to such implication of macroscopic softening behavior in our lattice model for concrete.

In particular, the meso-scopic brittle response is assumed to be caused only by the tensile failure of mortar members. Thus, the stress-strain relationships for the members of mortar and aggregate-mortar interface are idealized as elastic-brittle with breaking threshold f^t as shown in **Fig. 3**, while aggregate members are always assumed to have a linearly elastic property and not to fail. We also assume that the tensile strength of aggregate-mortar interface is only thee one fifth of that of mortar. In such material modeling for concrete, each meso-scopic lattice member never undergo compressive and shear failure. Instead, microcracks, which are represented by the removal of mortar or aggregate-mortar interface members, are activated only by *tensile* force to invite shear or splitting cracks even for macroscopically compressive loading.

b) Reinforcing steel and steel-concrete interface

A reinforcing steel bar is discretized into a series of steel members, which is the same network of truss elements as concrete members, and whose material nonlinearity is also idealized by a 1-D constitutive model. The classical one-dimensional rate-independent plasticity with isotropic bi-linear hardening, which is illustrated in **Fig. 4**, is employed for the constitutive model for steel members. Note again that the plastic deformation in our modeling does not exhibit softening behavior.

The influence of bonding characteristics between steel and concrete should not be neglected to express the failure of reinforced concrete structures. Several macro-scopic bond-slip relationships are obtained by pull-out tests; see, for example, Salem and Maekawa[16]. Yet, actual bond effects seem to be caused by the contact and the non-reversible behavior together with friction between steel and surrounding concrete. In this study, we try to capture such an effect by introducing the members of steel-concrete interface located between mortar and steel, as illustrated in **Fig. 5**. For simplicity, the interface region is also approximated by truss members whose mechanical behavior is characterized by the same 1-D rate-independent plasticity model as that of steel members but with different parameters, σ_y, E and K.

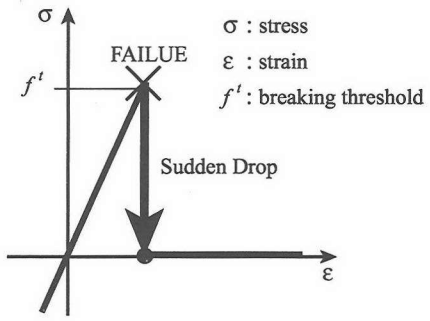

Fig. 3 Constitutive model for a mortar member

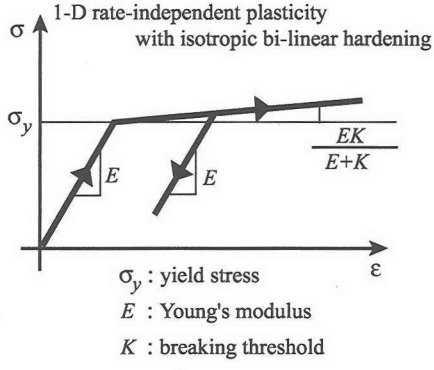

Fig. 4 Constitutive model for steel and steel-concrete interface members

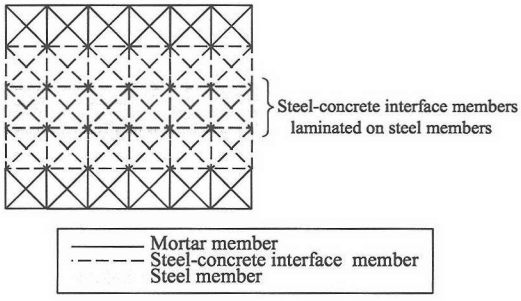

Fig. 5 Distribution of steel-concrete interface members

3. SIMULATION OF CONCRETE SPECIMENS UNDER BIAXIAL LOADING

In this section, we carry out the numerical simulation on a plane concrete specimen under biaxial loading (stress). The purpose of this simulation is to examine the performance of our modified lattice model with the DIB geometry modeling and, in particular, the capability to represent the fracture envelope under biaxial loading, which is one of the essential mechanical characteristics of concrete. A strategy of nonlinear analysis for lattice model is worked out in Appendix A.

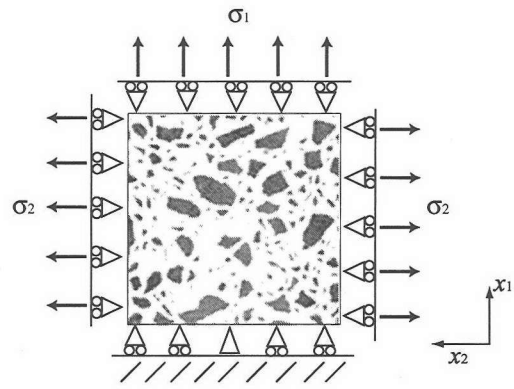

Fig. 6 Analysis model for biaxial loading

(1) Analysis model

We have prepared the analysis model and boundary conditions shown in **Fig. 6**. It is known that different boundary conditions of specimen lead to quite different failure modes and different apparent ultimate loads under compressive failure; see for example, Schlangen and Garboczi[14]. To avoid the effects of the friction at loading plane, the loading surfaces in the transverse directions are assumed to be stress free. Also, deformations in the perpendicular direction to the loading surfaces are assumed to be uniform.

The model is generated directly from a plane digital image of a cross-section (15 cm × 15 cm) of cylinderical specimen and has 150 × 150 finite elements (pixels). The resolution of the digital image is adjusted to 10 pixels/cm.

The material properties are chosen as follows: Young's modulus of mortar and interface members $E_m = 20\,\mathrm{GPa}$, that of coarse aggregate members $E_a = 60\,\mathrm{GPa}$, the breaking threshold for mortar is given by the tensile strain $\varepsilon_t^{\mathrm{m}} = 1.0 \times 10^{-4}$, and that for aggregate-mortar interface $\varepsilon_t^{\mathrm{i}} = 2.0 \times 10^{-5} (= \varepsilon_t^{\mathrm{m}}/5.0)$. Here, Young's modulus of each material are determined as the experimentally averaged values.

(2) Numerical result and discussion

Fig. 7 shows the apparent axial stress versus strain curves obtained by the simulations for uniaxial loading, and **Figs. 8, 9** and **10** show

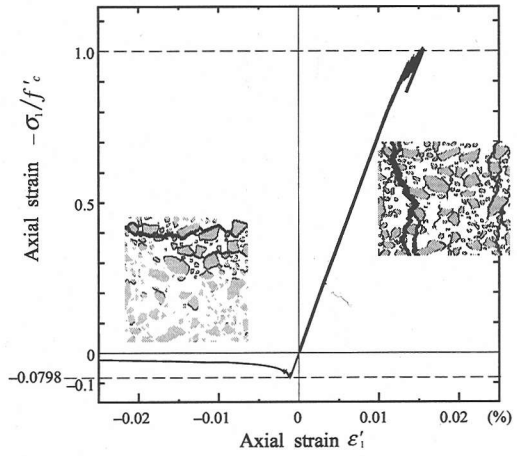

Fig. 7 Stress versus strain curves under uniaxial loading

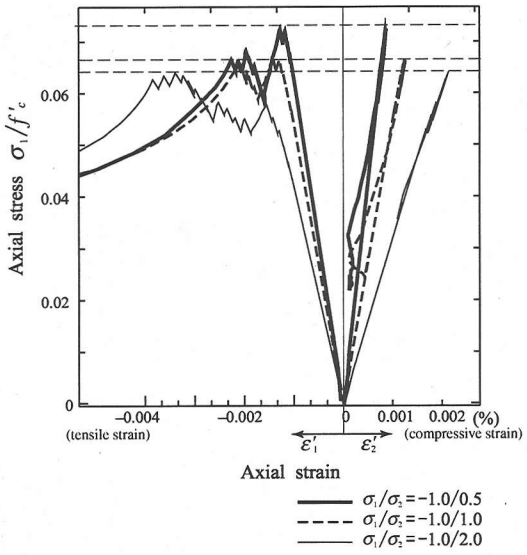

Fig. 8 Stress versus strain curves under biaxial loading ((σ_1)tension–(σ_2)compression domain)

the curves for biaxial loading. Especially, in the case of tension–tension domain and compression–tension domain, numerical result are compared with Kupfer's experimental result[17]. Here, the *apparent* means *macroscopically measured* as in actual experiments, and the stress and strain are respectively evaluated from the displacement and external force in the loading direction at the top surface. In these figures, the numerial and experimental axial stresses are normalized by the uniaxial compressive strength f'_c and σ_{co}, respectivelly. The features of experimental stress-strain relationship are qualitatively reproduced by this numrical simulations.

In **Fig. 11**, the strength, the maximum loading parameter, for each loading condition is plotted along with the fracture envelope under biaxial stress in the principal stress space. As for the fracture envelope, which is to be obtained through experiments, we have adopted Niwa model[18] derived for the compression–tension domain, Aoyagi-Yamada model[19] for the tension–tension domain and Kupher model[20] for the compression–compression domain. As can be seen from the figure, the strength characteristics evaluated in our simulations (shown by □) accord the well-known experimental trend with sufficient accuracy. The comparison in the compression–compression domain is not carrried out because our numerical simulation is limited to 2-D situation and, hence, cannot express the crack propagation only in the plane of x_1-x_2. Typical fracture modes after the post-peak region, which correspond to the points [a]∼[c] in **Fig. 11**, are shown in **Fig. 12**. As can be seen, the differences of fracture modes in the loading conditions are well captured.

It is emphasized here that the meso-scopic geometrical configuration in actual concrete plays an important role to capture such mechanical behavior. Note again that our lattice model does not involve compressive or shear failure criterions, but employs simple material models presented in Section 2.2.

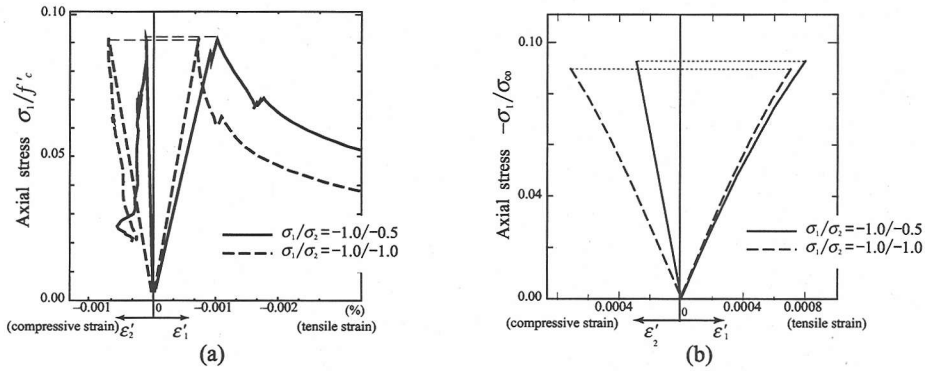

Fig. 9 Stress versus strain curves under biaxial loading ((σ_1)tension–(σ_2)tension domain) : (a) Numerical result, (b) Experimental results tested by Kupfer et al.[17]

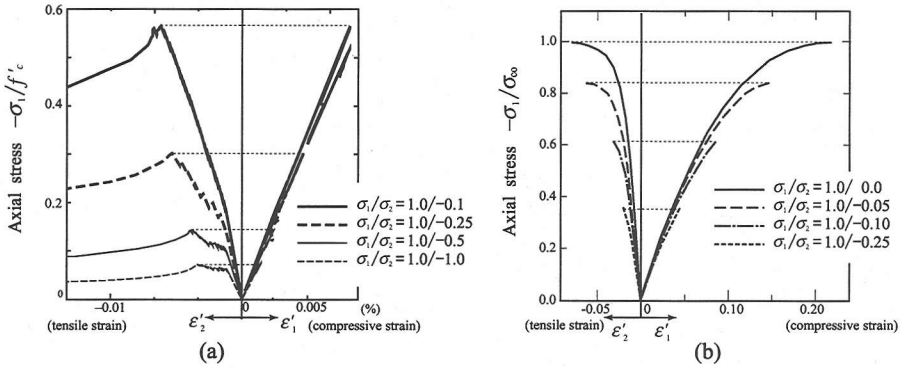

Fig. 10 Stress versus strain curves under biaxial loading ((σ_1)compression–(σ_2)tension domain) : (a) Numerical result, (b) Experimental results tested by Kupfer et al.[17]

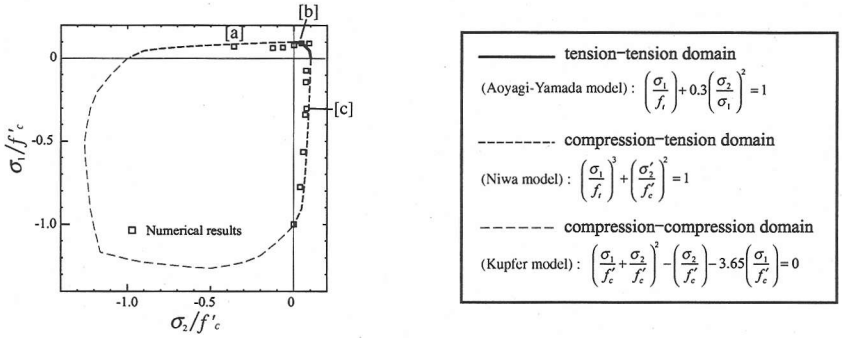

Fig. 11 Experimental and numerical fracture envelope of biaxial loading

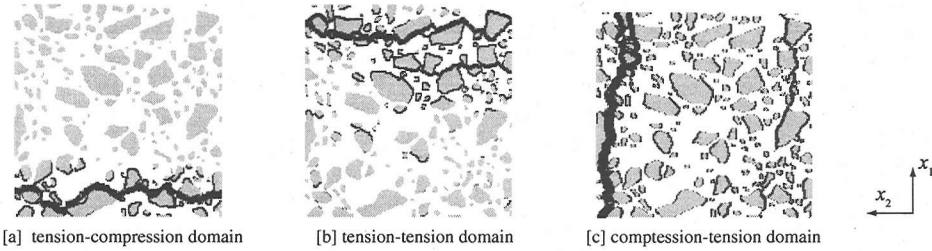

[a] tension-compression domain [b] tension-tension domain [c] comptession-tension domain

Fig. 12 Typical fracture modes under biaxial loading

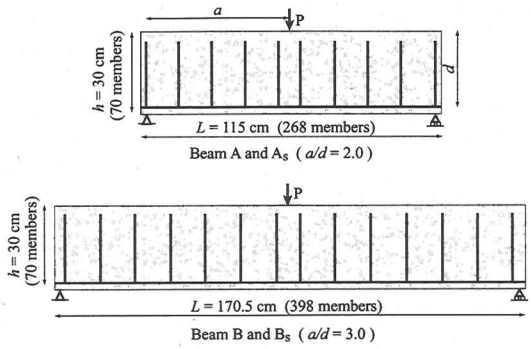

Fig. 13 Analysis models of concrete beams

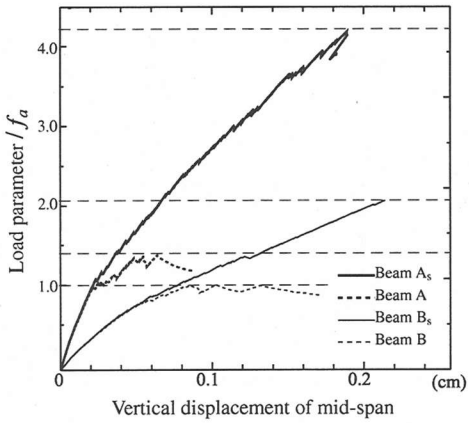

(a)

Fig. 14 Numerical result of load parameter versus vertical displacement curves at the loading point

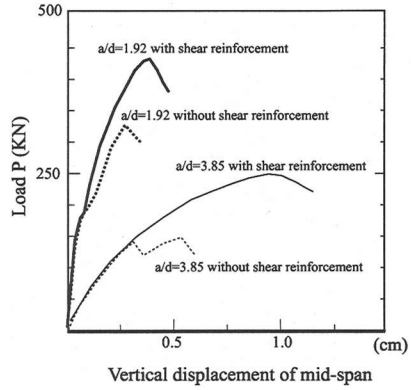

(b)

Fig. 15 Experimental load parameter versus vertical displacement relationships tested by Yamaya et al. [22]

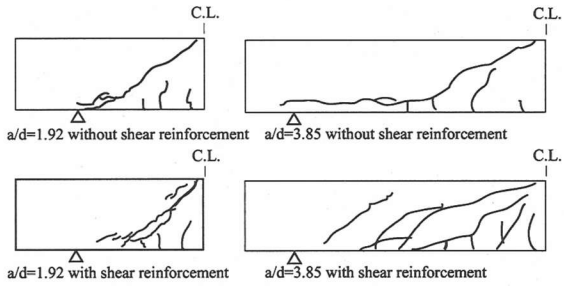

Fig. 16 Experimental cracking patterns at failure tested by Yamaya et al. [22]

4. SIMULATION OF REINFORCED CONCRETE BEAMS

The proposed analysis method is applied to the numerical analyses on a series of simply-supported reinforced concrete beams under a transverse point force at the midspan (three-point bending beams).

(1) Conditions of numerical simulations

Specimens with two different values of height-span ratio a/d (with the same effective depth d), and with and wihtout shear reinforcements are considered. The concrete is assumed to be of the same material composition as that employed in the previous section; see **Table 1** for physical properties employed.

The analysis models $\mathrm{A}, \mathrm{A_s}, \mathrm{B}$ and $\mathrm{B_s}$ in **Fig. 13** have been virtually generated by patching the digital images of the cross section of a concrete specimen. The dimensions of Beams A and B without shear reinforcements are chosen to be 30cm× 108cm and 30cm× 198cm, and a/d = 2.0 and 3.0, respectively. We further consider Beams $\mathrm{A_s}$ and $\mathrm{B_s}$ with the same dimensions but with the shear reinforcements. Here, the subscript $(\cdot)_s$ indicates the presense of shear reinforcements. The resolution of the digital image in this section is reduced from 10 pixel/cm to 2.5 pixel/cm in favor of the computational costs. Therefore, the mesh sizes of Beams A and B are identified with 75× 270 and 75× 570 elements, respectively.

(2) Numerical results

Fig. 14 shows the calculated curves for the loading parameter versus the vertical displacement at the point of loading P indicated in **Fig. 13**. The load parameter is normalized by the strength f_a for Beam A. **Figs. 15** and **16** show an exprimental load–displecement relationship and the cracking pattern at failure for com-

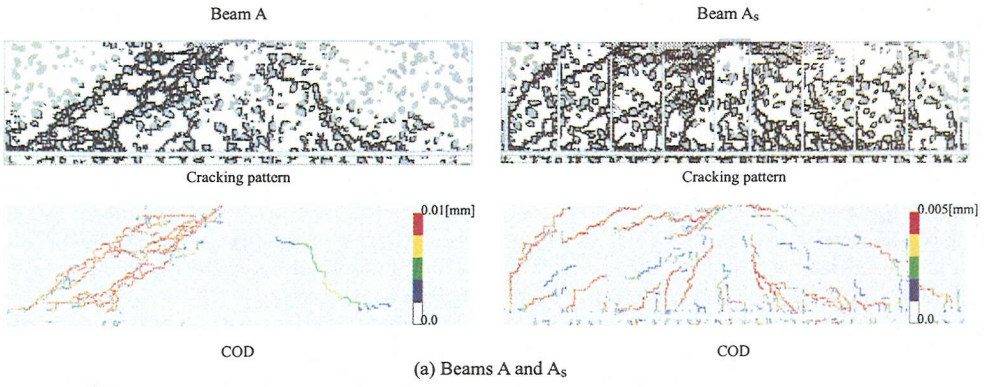

(a) Beams A and A_s

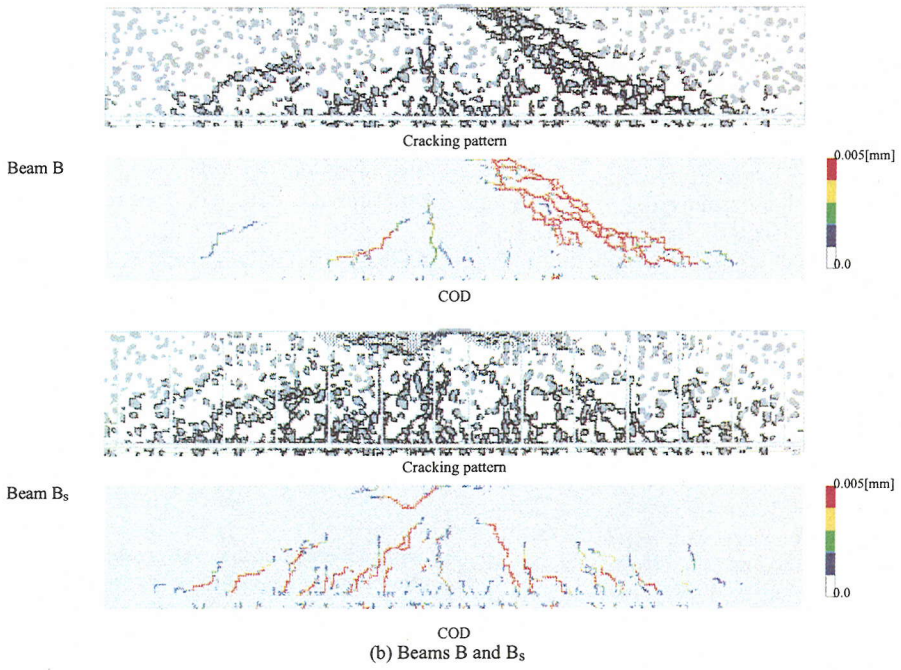

(b) Beams B and B_s

Fig. 17 Cracking patterns and COD at failure

Table 1 Physical properties

	Mortar	Aggregate	interface	Bond	Steel
E: young's modulus (GPa)	20	60	20	20	60
A: cross section area	1.0	1.0	1.0	1.0	1.0
ε_t: failure criterion	0.0001	-	0.00002	0.0001	-
ε_s: yield strain	-	-	-	(0.0001)	0.002
K: plastic hardening parameter	-	-	-	20	20

parison. Here, the size and the height-span ratio a/d of experimental spesimens are different from those used in the numerical simulation. The macro-scopic responses of the reinforced beams are characterized by the rugged lines, which are actually induced by the meso-scopic shear and splitting fracture of mortar members. Note that, owing to our modification of the method of inelastic force, see Appendix A, that was originally developed by Jirasek and Bažant[21], each equilibrated state is evaluated on a discrete loading step. As can be seen in **Fig. 14**, Beams A and A_s

exhibit much stiffer responses than Beam B and B_s, respectively. This is the well-known dependency of the apparent strength of reinforced concrete beams on the height-span ratio; as shown in **Fig. 15**. Also, Beams A_s and B_s reveal much stiffer response after the apparent yielding points and attain much higher peak loads than Beam A and B do, respectively. Actually, this is a typical effect of shear reinforcements, which is often reported in the literature; see, e.g., Leonhardt[23].

Numerical cracking patterns at failure with and without shear reinforcements are compared in **Fig. 17**. Crack Opening Displacement(COD) in this figure, which is approximately calculated by the distance between adjacent nodes, shows asymmetric fracture modes, especially for Beams A and B without shear reinforcements. Comparison of **Fig. 16** and **Fig. 17** shows the calculated cracking patterns look quite similar to the experimental ones.

Schlangen[24] reported that numerical results of lattice type models generally depend strongly on the failure criterion employed and the element and/or mesh type selected. In our proposed lattice model, on the contrary, the simple failure criterion, simple structural elements and the regular mesh, but with the accurate geometry modeling technique have been employed. Instead of the dependency on the fracture criterion inherent to lattice type models, the cracking patterns of macrocracks, which govern the stability of overall structure, are successfully simulated. That is, the mechanical behavior of reinforced concrete structures strongly depends on the meso-scopic heterogeneities and/or the interaction between steel and concrete, as well as the brittle nature of the meso-scale failure of mortar and aggregate-mortar interface. As a result of such capability to accurately simulate the actual phenomena, the complex (shear) failure modes of reinforced concrete structures have been simulated successfully.

5. CONCLUSIONS

We have presented a lattice type numerical model for the simulation of the quasi-static deformation of concrete and reinforced concrete structures. On the hypothesis that the macro-scopic softening behavior is the consequence of a series of local instabilities, we have incorporated the effect of meso-scale heterogeneities into the complex macro-scale mechanical behavior. In particular, our numerical concrete model is composed of as many as five regions (members); mortar, coarse aggregate, aggregate-mortar interface, steel and steel-concrete interface. The actual meso-scale heterogeneities is accommodated by means of the digital image-based modeling technique.

Numerical results for concrete specimens and reinforced concrete beams show the possibility that the fracture mechanisms of concrete material, which are conventionally interpreted as material instability from the macro-scopic viewpoits, can be interpreted as their meso-scale structural instability (cracking behavir). This suffices to ensure the validity of the aforementioned hypothesis. Thus, the following two significant aspects of our numerical concrete modeling strategy are again emphasized:

1. representation of the actual meso-scale *heterogeneities*, and
2. characterization of the meso-scale *localization* behavior without complex constitutive modeling.

In conclusion, this type of numerical models is effective to some extent, especially for the qualitative studies of the relationship between the localized deformations due to heterogeneities and the stability of concrete structures. The calibration of model parameters in view of a series of experimental data will be a topic in the future.

ACKNOWLEDGMENT: The support of the staffs of Structural Engineering Laboratory in the department of civil engineering at Hiroshima Univ. is much appreciated.

Appendix A NONLINEAR ANALYSIS METHOD FOR LATTICE TYPE MODEL

In this appendix, we present a nonlinear analysis method for lattice type numerical models with geometrical nonlinear effect. By this technique, highly complex equilibrium paths caused by the material and geomerical nonlinearity can be traced stably. The analysis procedure is similar to that of the method of inelastic force (MIF), which was originally proposed by Jirasek and Bažant[21] for the dynamic motion of cracking. In the present study, however, we try to attain the quasi-static equilibrium states of concrete structures by using the Newton-Raphson iterative scheme with the arc-length control. In particular, to characterize the brittle mechanical response of mortar members, our numerical analysis method is established by the concept of operation splitting as shown in **Fig. 18**. That is, our analysis scheme has two successive steps as follows.

1. In the first step, we obtain the fictitious equilibrium state, in which the mortar members deform elastically and do not fail. Also, the steel and bond members are assumed to undergo only elastic-plastic deformation. The analysis, accordingly, is completely conven-

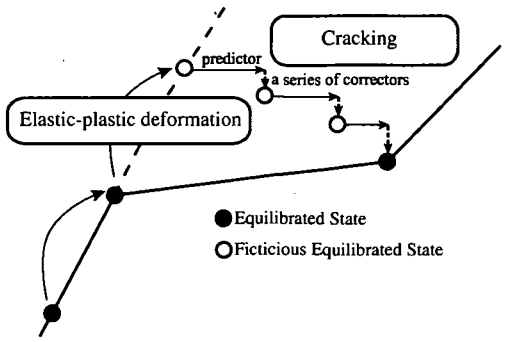

Fig. 18 Concept of operation splitting

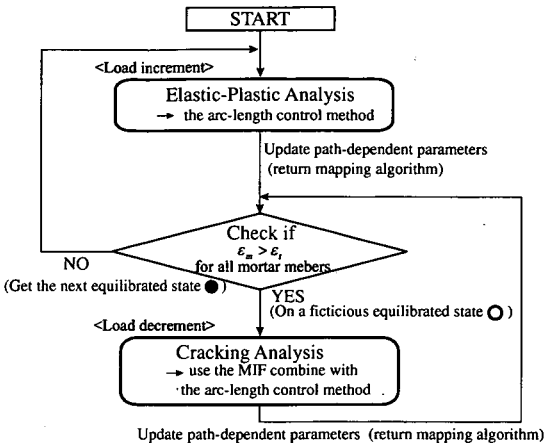

Fig. 19 Flow chart of analysis

tional and one can refer to the standard textbook for computations; see, e.g., Simo and Hughes[25].

2. The second step is implemented to perform the cracking analysis with inelastic force to attain the actual equilibrium state after cracking. When some mortar members exceed a breaking threshold, the subsequent equilibrium states are sequentially sought with released forces until the new cracking does not occur. On the other hand, the fictitious state becomes a true one if there are no mortar members that exhibit cracking.

Though the first phase is trivial, the further explanation for actual computations is given in the following. The internal force associated with the failure of mortar members is regarded as a releasing force, which would triggers new failure. The releasing force $\boldsymbol{f}_{\text{rel}}$ can be written as

$$\boldsymbol{f}_{\text{rel}} = \bigcap_{m=1}^{M} \boldsymbol{r}'_m \qquad \text{(A.1)}$$

where $\boldsymbol{r}'_m$ is the elementary internal force vector for a single member, $\bigcap$ indicates the special operator to assemble only from newly broken members. We solve the following linearized equilibrium equation to obtain the incremental displacement $\mathrm{d}\boldsymbol{u}$:

$$\boldsymbol{K}\,\mathrm{d}\boldsymbol{u} = \boldsymbol{f}_{\text{rel}} \qquad \text{(A.2)}$$

where $\boldsymbol{K}$ is the global tangent stiffness matrix assembled from element stiffness matrix of not-broken members. Here, the loading pattern vector of the conventional Newton-Raphson scheme has been replaced by the releasing force in this second step. Regarding the solution $\mathrm{d}\boldsymbol{u}$ as a predictor, we seek the next fictitious state by the arc-length method. This process is repeated until the actual equilibrium state is obtained. The flow chart of the analysis is shown in **Fig. 19**.

REFERENCES

1) Zaitsev, Y. B. and Wittmann, F. H.: Simulation of crack propagation and failure of concrete, *Materals and Construction*, Vol.14, pp.357–365, 1981.
2) Bhatt, P. and Adbel-Kader, M.: Prediction of shear strength of reinforced concrete beams by nonlinear finite element analysis, *Computers and Structures*, Vol.68, pp.139–155, 1998.
3) An, X. and Maekawa, K.: Numerical simulation on shearfailure of RC beams, *Fracture Mechanics of Concrete Structures*, Proceedings of FRAMCOS-3, AEDIFICATIO Publishers, Germany, pp.1077–1086, 1998.
4) Bažant, Z. P. and Oh, B. H.: Crack band theory for fracture of concrete, *Material and Structures*, Vol.16, No.93, pp.155–177, 1983.
5) Bažant, Z. P., Tabbara, M. R., Kazami, M. T. and Cobat, G. R.: Random particle model for fracture of aggregate or fiber composites, *Journal of Engineering Mechanics*, ASCE, Vol.116, No.8, pp.1686–1705, 1990.
6) Schlangen, J. M. and van Mier, J. G. M.: Simple lattice model for numerical simulation of fracture of concrete materials and structures, *Materials and Structures*, Vol.25, pp.534–542, 1992.
7) Nagai, G., Yamada, T. and Wada, A.: Stress analysis of concrete material based on geometrically accurate finite element modeling, *Fracture Mechanics of Concrete Structures*, Proceedings of FRAMCOS-3, AEDIFICATIO Publishers, Germany, pp.1077–1086, 1998.
8) Kwan, A. K. H., Wang, Z. M. and Chan, H. C.: Mesoscopic study of concrete II: nonlinear finite element analysis, *Computers and Structures*, Vol.70, pp.545–556, 1999.
9) Cundall, P. A. and Strack, O. D. L.: A discrete numerical model for granular assemblies, *Geotechnique*, Vol.29, pp.47–65, 1979.
10) Zubelewicz, A.: Contact element method, Ph.D Thesis, The Technical University of Warsaw, Poland, 1980.
11) Zubelewicz, A. and Mróz, Z.: Numerical simulation of rockburst processes treated as problems

of dinamic instability, *Rock Mechanics and Engineering*, Vol.16, pp.253–274, 1983.
12) Hollister, S. J. and Kikuchi, N.: Homegenization theory and digital imaging: a basis for the mechanics and disign principles of bone tissue, *Biotechnology and Bioengineering*, Vol.32, No.1, pp.27–62, 1994.
13) Terada, K., Miura, T. and Kikuchi, N.: Digital image-based modeling applied to the homegenization analysis of composite materials, *Computational Mechanics*, Vol.20, pp.331–346, 1997.
14) Schlangen, E. and Garboczi, E. J.: Fracture simulations of concrete using lattice models: computational aspects, *Engineering Fracture Mechanixs*, Vol.57, No.2/3, pp.319–332, 1997.
15) Drescher, A. and Vardoulakis, I.: Geometric softeing in triaxial tests on granular material, *Geotechnique*, Vol.32, No.4, pp.291–303, 1982.
16) Salem, H. M. and Maekawa, K.: Coupled bond and bridging stress transfer in cracked reinforced concrete, *Fracture Mechanics of Concrete Structures*, Proceedings of FRAMCOS-3, AEDIFICATIO Publishers, Germany, pp.1353–1362, 1998.
17) Kupfer, H., Hilsdorf, H. K. and Rusch, H.: Behavior of concrete under biaxial stresses, *ACI Journal*, Vol.66, No.8, pp.656–666, 1969.
18) Niwa, J., Yamada, K., Yokozawa, K. and Okamura, H.: Reveluation of the equation for shear strength of reinforced concrete beams without web reinforcement, *Concrete Library of JSCE*, No.9, pp.65–84, 1987.
19) Aoyagi, Y. and Yamada, K.: Strength and deformation characteristics of reinforce concrete shell elements sucjected to in-plane forces, *Proc. of JSCE*, No.331, pp.167–180, 1983.
20) Kupfer, H. B. and Gerstle, K. H.: Behavior of concrete under biaxial stresses, *Proc. of ASCE*, EM4, pp.853–866, 1973.
21) Jirasek, M. and Bažant, Z. P.: Macroscopic fracture characteristic of random particle systems, *International Journal of Fracture*, Vol.69, pp.201–228, 1995.
22) Yamaya, A., Nakamura, H. and Higai, T.: Shear behavior analysis of RC beams using rotating crack model, *Journal of Matrials, Concrete Structures and Pavements, JSCE*, No. 620/V-43, pp.187–199, 1999. (In Japanese)
23) Leonhardt, F.: Reducing the shear reinforcement in reinforced concrete beams and slabs, *Magazine of Concrete Research*, Vol.17, No.53, pp.187–198, 1965.
24) Schlangen, E.: Computational aspects of fracture simulations with lattice models, *Fracture Mechanics of Concrete Structures*, Proceedings of FRAMCOS-2, AEDIFICATIO Publishers, Freiburg, pp.913–927, 1995.
25) Simo, J. C. and Hughes, T. J. R.: *Computational Inelasticity*, Springer-Verlag New York, Inc., 1998.

(Received April 15, 2002)

ラチスモデルによるコンクリート構造のメゾレベル解析

浅井 光輝・寺田 賢二郎・池田 清宏・陶山 裕之・藤井 堅

本研究では，材料の破壊プロセスの追跡，あるいは破壊モード予測手法として定評のあるラチスモデルに着目し，RC 構造までの破壊現象までを再現できるよう修正を加えた解析手法を提案し，数値解析を通してその適用性の検証を行った．本解析手法では，RC 構造をモルタル，粗骨材，骨材界面，鉄筋そして鉄筋界面の 5 つの領域に分類し，各領域ごとに単純な材料モデルを与えることにした．また，コンクリート材料におけるモルタルと骨材の非均質な幾何形状を正確に表現するために，コンクリート断面の実画像から解析モデルを作成した．数値解析では，コンクリート材料試験から RC 構造までの広汎な解析対象に対しても現実的なクラック進展挙動が再現されている．